Davis, Clare E.; Mahaffey, Claire; Wolff, George A.; Sharples, Jonathan. 2014 A storm in a shelf sea: Variation in phosphorus distribution and organic matter stoichiometry. *Geophysical Research Letters*, 41 (23). 8452-8459. 10.1002/2014GL061949

Davis, Clare E.; Mahaffey, Claire; Wolff, George A.; Sharples, Jonathan. 2014 A storm in a shelf sea: Variation in phosphorus distribution and organic matter stoichiometry. *Geophysical Research Letters*, 41 (23). 8452-8459. 10.1002/2014GL061949

AGU PUBLICATIONS

Geophysical Research Letters

RESEARCH LETTER
10.1002/2014GL061949

Key Points:
- Storm enhanced phosphate fluxes stimulate net production of organic matter
- Phosphorus-rich dissolved organic matter exported below thermocline
- Particles become more efficient at transferring carbon relative to phosphorus

Correspondence to:
C. E. Davis,
davis@liverpool.ac.uk

Citation:
Davis, C. E., C. Mahaffey, G. A. Wolff, and J. Sharples (2014), A storm in a shelf sea: Variation in phosphorus distribution and organic matter stoichiometry, *Geophys. Res. Lett.*, *41*, 8452–8459, doi:10.1002/2014GL061949.

Received 19 SEP 2014
Accepted 7 NOV 2014
Accepted article online 11 NOV 2014
Published online 2 DEC 2014

A storm in a shelf sea: Variation in phosphorus distribution and organic matter stoichiometry

Clare E. Davis[1], Claire Mahaffey[1], George A. Wolff[1], and Jonathan Sharples[1,2]

[1]Department of Earth, Ocean, and Ecological Sciences, University of Liverpool, UK, [2]National Oceanography Centre, Liverpool, UK

Abstract Organic matter (OM) plays an important role in productive shelf seas and their contribution to global carbon (C) and nutrient cycles. We investigated the impact of storm mixing on OM dynamics in the seasonally stratified Celtic Sea. After the storm, OM production was decoupled from consumption in the euphotic layer. Over the 15 day study, dissolved OM (DOM) became phosphorus (P) rich relative to C, whereas particulate OM (POM) became P-deplete relative to C. Upward diapycnal phosphate fluxes were accompanied by reciprocal downward mixing of dissolved organic P (DOP) and particulate P (PPhos). Transfer of DOP and PPhos below the thermocline accounts for 22% and 26%, respectively, of the upward phosphate flux. Given the changes in stoichiometry of POM and DOM after the storm, the form in which OM is transferred below the thermocline has important implications for the efficiency of elemental transfer, impacting C cycling and storage in the ocean.

1. Introduction

Shelf seas represent less than 10% by area of the global ocean, yet are responsible for 15 to 30% of its primary production and up to 50% of the export production [*Wollast,* 1998]. The driving forces behind the highly productive nature of shelf seas are the relatively rich nutrient supply from adjacent terrestrial and oceanic sources and the amplification of tidal- and wind-driven mixing relative to the deeper open ocean [*Thomas et al.,* 2004]. The annual cycle of primary production in temperate shelf seas is dominated by a relatively short spring bloom and then weaker but more sustained subsurface chlorophyll maxima (SCM) that develops within the base of the seasonal thermocline during summer stratification. Annually, these draw down approximately equal amounts of carbon (C) from the atmosphere [*Hickman et al.,* 2012]. The SCM is sustained by a diapycnal nutrient flux across the base of the thermocline, which is sensitive to tidal- [*Sharples et al.,* 2007] and wind- [*Williams et al.,* 2013b] driven mixing processes. Recent field studies have highlighted the importance of storms or wind events in enhancing these diapycnal nutrient fluxes [e.g., *Tweddle et al.,* 2013] and sustaining summertime productivity [*Williams et al.,* 2013b].

Although enhanced productivity and change in community structure have been observed, the fate of dissolved and particulate organic material (DOM and POM, respectively) after such storm events is still unclear. DOM and POM are biologically produced in the euphotic layer [*Carlson,* 2002]. During bloom events, production of organic matter (OM) is often decoupled from consumption leading to an accumulation in surface waters [*Hydes et al.,* 2001; *Wetz and Wheeler,* 2003], and thus the production of DOM and POM is strongly regulated by primary production [*Carlson,* 2002]. DOM and POM act as important vehicles for nutrient transfer between the sunlit surface layer and dark deeper layers of the ocean. Microbial processes strongly influence the stoichiometry and lability of OM [*Azam et al.,* 1983; *Martiny et al.,* 2013], which determines if DOM and POM act as C and energy sources for heterotrophs, nutrient sources for autotrophs, or are exported off-shelf [*Hopkinson et al.,* 1997; *Lønborg and Alvarez-Salgado,* 2012].

Here, we report on observations made around the relatively shallow area of Jones Bank (<100 m) in the Celtic Sea (Figure 1a). The influence of topography and internal tides on biogeochemical signals was masked by the impact of a significant wind-driven mixing event that greatly enhanced vertical mixing and transported nutrients into the surface mixed layer. In the Celtic Sea, nitrogen (N) limits primary production [e.g., *Pemberton et al.,* 2004] and therefore changes in the labile and semi-labile fractions of the DOM pool are more readily measurable in the phosphorus (P) pool which gives greater insight into the stages of OM cycling. Here we report the changes in distribution and partitioning of P in the euphotic layer and estimate vertical diapycnal nutrient fluxes across the base of the thermocline during a 15 day sampling campaign after a strong wind-mixing event.

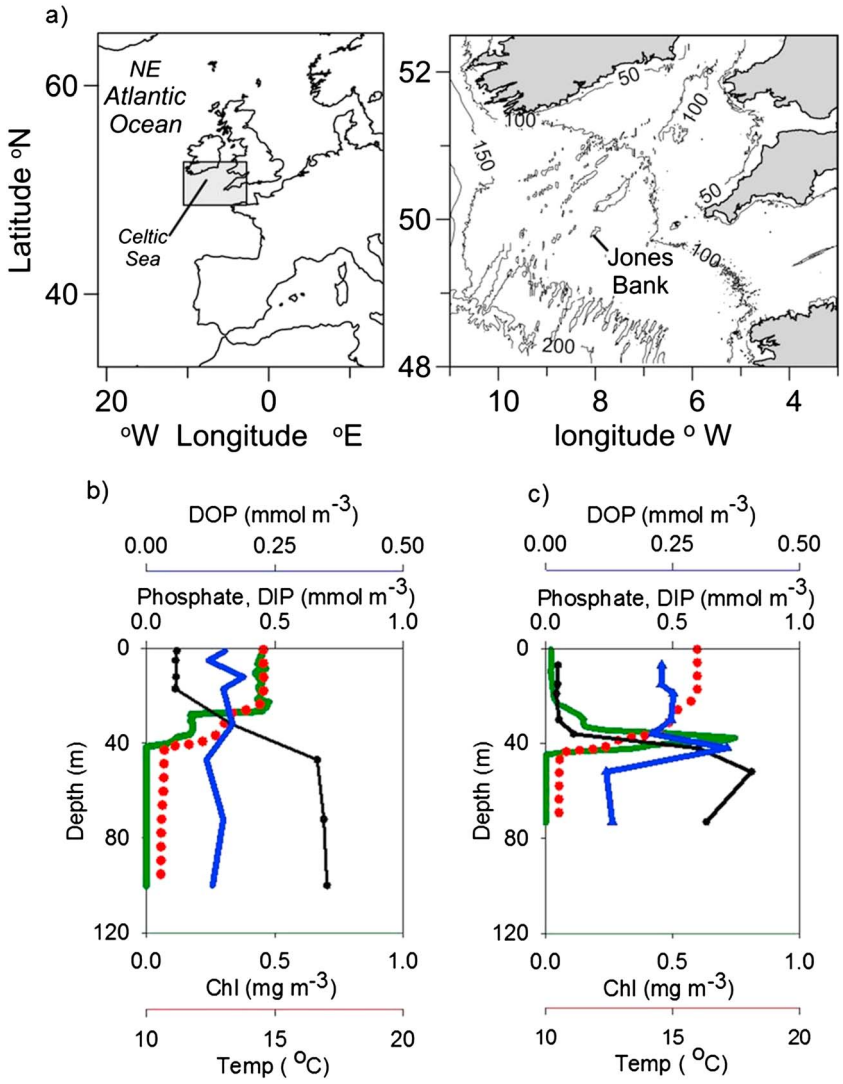

Figure 1. (a) Location and bathymetry of Jones Bank region of the Celtic Sea, NW European shelf, taken from *Sharples et al.* [2013]; (b) vertical profiles of chlorophyll *a* (green), temperature (red), phosphate (dissolved inorganic phosphate (DIP); black), and dissolved organic phosphorus (DOP; blue) at stormy spring tide (day 187), and (c) the calm spring tide (day 202).

2. Methods

Samples were collected from the *RRS James Cook* (cruise JC025) during a spring-neap-spring tidal cycle in the Celtic Sea located on the NW European shelf in the Jones Bank region (Figure 1a; 49.75 – 50.0°N, 07.65 – 8.175°W). The sampling campaign, (6–21 July 2008, decimal days 187 to 202) consisted of measurements of vertical profiles of temperature, turbulent kinetic energy dissipation [*Palmer et al.,* 2013], and collection of samples for analysis of inorganic phosphate, organic P, chlorophyll *a* (hereafter chl *a*), particulate nutrients, and rate of alkaline phosphatase activity (hereafter APA).

2.1. Hydrography, Chlorophyll *a*, Nutrients, and Phosphorus Cycling

A rosette frame, supporting a Seabird 911 conductivity, depth, temperature (CTD) instrument, a fluorometer, and 20 L Niskin bottles was used to collect vertical profiles of salinity, temperature, chl *a* fluorescence, and seawater samples. Methods for analysis of chl *a* using acetone extraction, phytoplankton numeration and identification, and rates of primary production are described in *Davidson et al.* [2013].

Seawater samples were filtered through Whatman glass fiber filter (GF/F, 0.7 μm pore size, precombusted at 450°C for 4 h prior to acid washing, deionized water rinsing, and drying at 50°C) and stored in 250 mL bottles

(acid-washed, HDPE Nalgene) at −20°C prior to determination of dissolved inorganic phosphate (DIP) as in *Williams et al.* [2013b]. Total UV-oxidizable dissolved organic phosphorus (DOP) and phosphomonoester (PME) concentrations were determined as in *Reynolds et al.* [2014]. Concentrations of dissolved organic carbon (DOC) and dissolved organic nitrogen (DON) were determined by high temperature catalytic oxidation, and dissolved inorganic nitrogen (DIN) was determined by standard colorimetric techniques [*Davidson et al.,* 2013].

Particulate phosphorus (PPhos) concentrations were determined by filtering 1 L of seawater onto a Whatman glass fibre filter (GF/F, 0.7 μm pore size, precombusted, and acid washed as above). PPhos was determined by DIP analysis as above, following high-temperature combustion and hydrochloric acid extraction [*Karl et al.,* 2001]. Particulate organic carbon (POC) and particulate nitrogen (PN) concentrations were determined by filtering 2 L of seawater onto a Whatman glass fiber filter (GF/G, 0.7 μm pore size, precombusted). POC and PN were analyzed after vapor phase decarbonation using a Carlo Erba Elemental Analyzer [*Yamamuro and Kayanne,* 1995].

Alkaline phosphatase activity (APA) was used to determine the potential enzyme-mediated turnover of the most labile fraction of the DOP pool. APA rates were determined in unfiltered seawater samples according to methods described by *Ammerman* [1993] and *Sohm et al.* [2008], using the synthetic PME compound (methylumbelliferyl-phosphate) at a concentration range between 800 and 2000 nM, and rates were determined at the saturating substrate concentration.

2.2. Flux Calculations

Using the turbulent kinetic energy dissipation data collected during JC025 [*Tweddle et al.,* 2013; *Palmer et al.,* 2013], P fluxes across the base of the thermocline were estimated [*Sharples et al.,* 2007], for example for phosphate, using the following equation:

$$PO_4^{3-}\,flux = -Kz\left(\frac{\delta PO_4^{3-}}{\delta z}\right) mmol\ \ m^{-2}s^{-1}$$

where Kz is eddy diffusivity at the base of the thermocline in $m^2\,s^{-1}$, and $\delta PO_4{}^{3-}$ is the vertical phosphate concentration gradient across the base of the thermocline in mmol m^{-3} and δz is change in depth across the gradient in m.

3. Results and Discussion

3.1. Water Column Structure

The water column maintained a three-layer structure with temperature dominating density throughout the study (Figures 1b and 1c), despite the occurrence of a storm where wind speeds reached over 50 knots (day 185; Figures 2a and 2b) driving enhanced vertical mixing at the thermocline. *Palmer et al.* [2013] record average thermocline vertical diffusivities of $1.9\times10^{-3}\,m^2\,s^{-1}$ during initial sampling conducted during the stormy spring tide, compared with $2.8\times10^{-5}\,m^2\,s^{-1}$ on the neap tide and $3.3\times10^{-4}\,m^{-2}\,s^{-1}$ on the later calm spring tide. The dominance of storm-generated mixing over topographically induced internal wave mixing at the bank meant that there were no significant spatial trends, but that the temporal trend of "post-storm" recovery of the water column dominated the measured biogeochemical patterns [*Davidson et al.,* 2013; *Sharples et al.,* 2013; *Tweddle et al.,* 2013]. This is also reflected in the chl *a* fluorescence distributions, which show entrainment and mixing through the euphotic layer during the earlier period of strong mixing and later show that the SCM developed associated with the base of the thermocline (Figure 2c).

3.2. A Simple Phosphorus Budget for the Euphotic Layer

3.2.1. Observed Changes in the Euphotic Layer

Nutrient concentrations and rates of P cycling were integrated across the euphotic layer, which was considered to be the SML and thermocline combined (Figure 3). During the sampling period (decimal days 187 to 202) the average DIN:DIP ratio was ~13:1 in the bottom mixed layer, which was lower than the Redfield ratio of 16:1, [*Redfield et al*., 1963] implying that productivity in this region is limited by the availability of N. During the study, the net DIP drawdown rate was 0.41 mmol $m^{-2}\,d^{-1}$ from 11.5 to 5.3 mmol m^{-2} (Figure 3a; *R* 0.90, *p* 0.002), and net PPhos consumption rate was 0.28 mmol $m^{-2}\,d^{-1}$ from

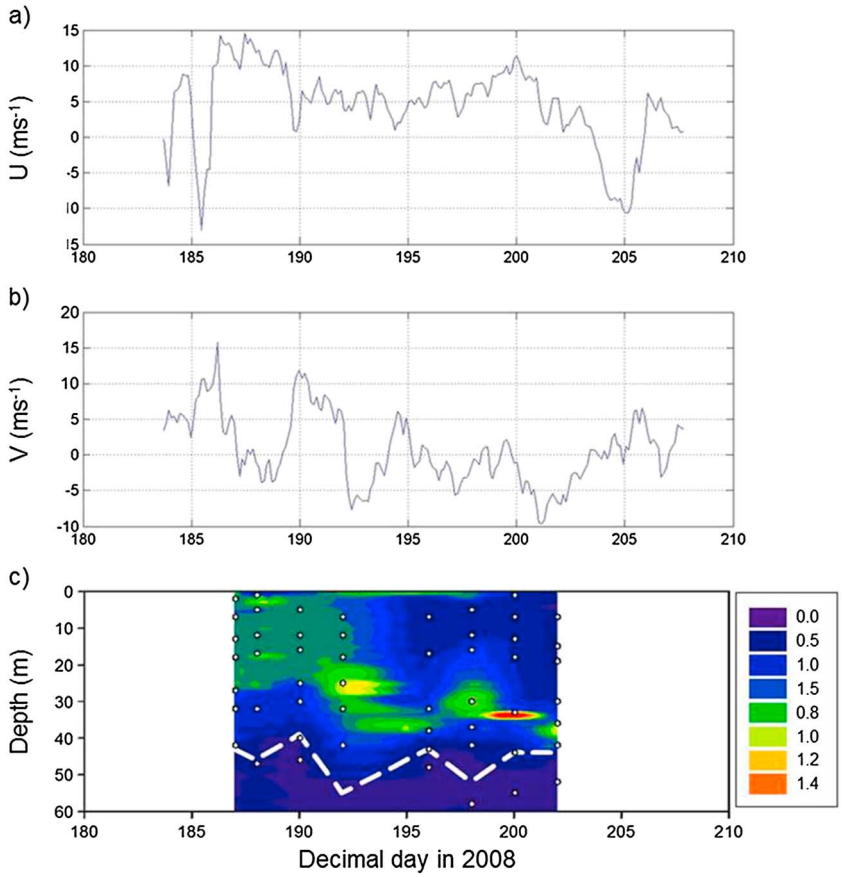

Figure 2. (a) Temporal *u* velocity wind component (m s^{-1}), positive indicates eastward air currents; (b) temporal *v* velocity wind component (m s^{-1}), positive indicates northward air currents; (c) temporal depth distribution of calibrated chlorophyll *a* fluorescence (μg L^{-1}): the white dashed line indicates the depth of the base of the euphotic layer, and the white dots indicate sampling intervals within the upper 60 m of the water column.

5.8 to 1.6 mmol m^{-2} (Figure 3c; *R* 0.78, *p* 0.022), while the net DOP production rate was 0.37 mmol m^{-2} d^{-1} from 6.1 to 11.8 mmol m^{-2} (Figure 3b; *R* 0.90, *p* 0.003), suggesting that DOP production exceeded PPhos consumption but was less than the DIP drawdown rate. The net loss rate of P from the euphotic layer was 0.32 mmol m^{-2} d^{-1} (Figure 3d; *R* 0.66, $p = 0.03$) during the study. APA from 0.01 mmol P m^{-2} d^{-1} to 0.03 mmol P m^{-2} d^{-1} (*R* 0.63, *p* 0.097; data not shown).

DOM nutrient ratios changed from 416C:33 N:P (day 187) to 281C:17 N:P (day 202), with the DOC:DOP and DON:DOP ratios decreasing linearly (Figure 3e; 0.94, *p* 0.0006; *R* 0.86, *p* 0.013, respectively), indicating that the euphotic layer DOM pool was becoming progressively P rich relative to C and N during the study period. Meanwhile, in the particulate pool, nutrient ratios changed from 63C:10 N:P (day 187) to 223C:38 N:P (day 202), with the POC:PPhos and PN:PPhos ratios increasing linearly during the study (Figure 3f; *R* 0.74, *p* 0.038 and *R* 0.76, *p* 0.067, respectively). This suggests that the euphotic layer POM pool was becoming progressively P depleted due to preferential release of P in the surface water [*Faul et al.,* 2005]. The accumulation of P in the dissolved organic phase relative to C and N combined with the preferential release of P from the particulate phase suggests that the increase in DOP is likely via solubilization and release from the particulate pool within the euphotic layer [*Antia,* 2005].

Rates of biological remineralization of the labile PME fraction of DOP were very low (0.2 – 1.3 nM P d^{-1}) with the equivalent of ~0.5 mmol PME m^{-2} being remineralized during the study, which means that <0.5% of euphotic layer integrated DOP was remineralized per day. The observed increase in APA may be linked to increased bacterial abundance [*Davidson et al.,* 2013]; thus, the APA may have been constitutive rather than induced in response to P-stress, which may explain why the observed remineralization rates were so low

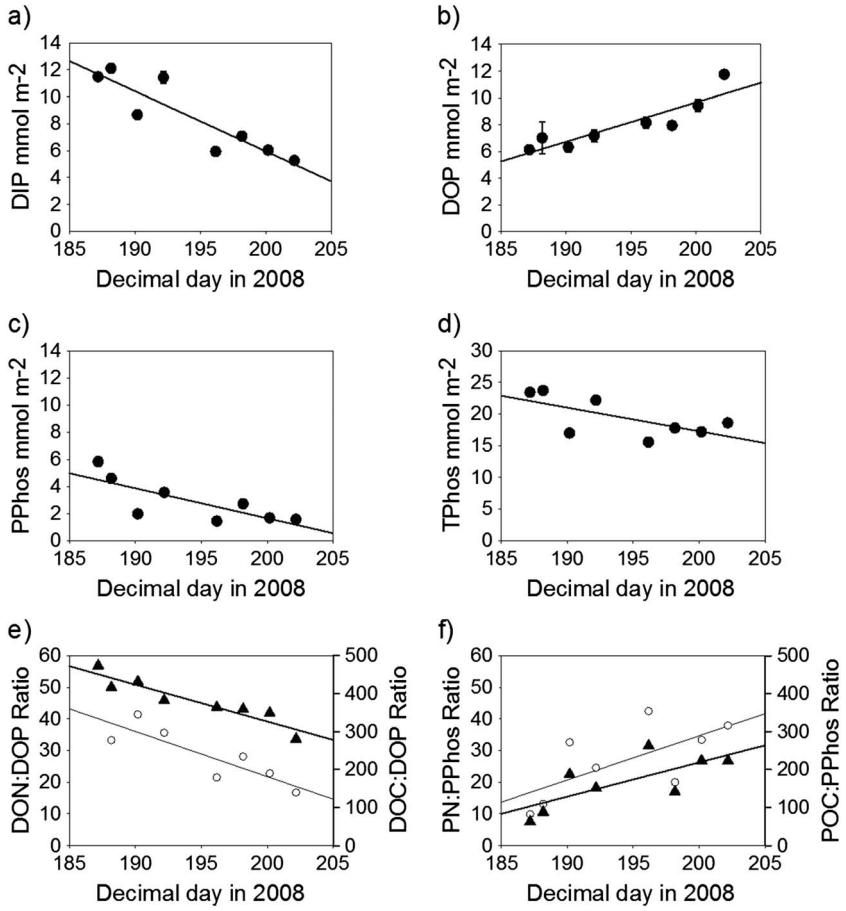

Figure 3. Temporal variation in euphotic layer integrated nutrient concentrations (mmol m^{-2}; error bars represent 95% confidence intervals) in (a) phosphate, DIP (DIP = −0.5 × +95, $p = 0.002$); (b) dissolved organic phosphorus, DOP (DOP = 0.3 × –49, $p = 0.003$); (c) particulate phosphorus, PPhos (PPhos = −0.2 × +46, $p = 0.02$); (d) total phosphorus, TPhos (TPhos = −0.4 × +92, $p = 0.03$); (e) dissolved organic matter stoichiometry (C:P triangles (C:P = −9.7 × +2270, $p = 0.0002$), N:P open circles (N:P = −1.4 × +308, $p = 0.009$)); (f) particulate organic matter stoichiometry (C:P triangles (C:P = 9.0 × –1585, $p = 0.05$), N:P open circles (N:P = 1.4 × –245, $p = 0.09$)).

[*Ruttenberg and Dyhrman,* 2005]. Given that there was no rapid turnover of this DOP in the euphotic layer, we suggest that there was a decoupling of DOP production and consumption that allowed DOP to accumulate, as has been observed elsewhere [*Ruttenberg and Dyhrman*, 2012; *Reynolds et al.,* 2014].

The decrease in DIP was likely driven by assimilation associated with primary production in the euphotic layer, which was reported to decrease linearly with time after the storm from ~400 mg C m^{-2} d^{-1} to ~240 mg C m^{-2} d^{-1} [*Davidson et al.,* 2013]. Primary production would act to transfer P from the DIP to the PPhos pool via assimilation. Assuming Redfield stoichiometry of 106C: 1P, the observed primary production [*Davidson et al.,* 2013] would require approximately 2.8 mmol P m^{-2} during the 15 day study, which is approximately half of the observed 6.2 mmol m^{-2} decrease in DIP. Additional sinks for DIP may have included adsorption to sinking particles [*Paytan and McLaughlin,* 2007] and loss below the thermocline associated with diel zooplankton vertical migration and grazing [*Steinberg et al.,* 2002]. The UV hydrolysis method is known to provide potentially poor recoveries for certain DOP compounds, such as ATP and polyphosphate, using the UV hydrolysis method [*Benitez-Nelson*, 2000], which may have resulted in poor recovery of DOP and therefore underestimation of the transfer of DIP to the DOP pool. Transfer from the POM to DOM pool may be a combination of passive exudation of P-rich DOM by diatoms [*Conan et al.,* 2007], which were dominant after the storm. Later zooplankton grazing and sloppy feeding and viral cell lysis may have been significant sources of DOP in the euphotic layer and at the SCM once the autotroph community became dominated by smaller species [*Davidson et al.,* 2013] that do not release DOM as readily [*Conan et al.,* 2007].

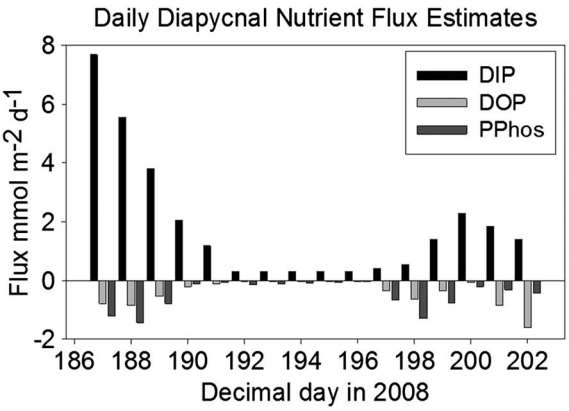

Figure 4. Daily diapycnal phosphorus flux estimates (mmol P m^{-2} d^{-1}) across the base of the thermocline for phosphate (DIP, black), dissolved organic phosphorus (DOP, grey), and particulate phosphorus (PPhos, dark grey). Positive values indicate an upward flux or supply to the euphotic layer, and negative values indicate a downward flux or loss from the euphotic layer.

Overall, the net consumption or loss rate from the DIP and PPhos pools during the study period were 0.41 ± 0.09 mmol m^{-2} d^{-1} and 0.28 ± 0.09 mmol m^{-2} d^{-1}, respectively, equivalent to a combined loss rate of 0.70 ± 0.18 mmol P m^{-2} d^{-1} in the euphotic layer. At the same time, DOP was produced or accumulated at a rate of 0.37 ± 0.20 mmol m^{-2} d^{-1}, representing 46% of the decrease in DIP and PPhos. This suggests that there was a net loss of 4.8 ± 0.14 mmol P m^{-2} from the euphotic layer over the 15 day study period, at a rate of 0.32 mmol P m^{-2} d^{-1}. This loss may have been driven by vertical mixing or lateral advection of organic P (collectively DOP and PPhos, herein OP).

3.2.2. Vertical Nutrient Fluxes

Shelf seas are physically dynamic regions and mixing across the base of the thermocline linked to wind- and tidally driven shear and turbulence is a ubiquitous feature of the stratified shelf sea [e.g., *Williams et al.,* 2013a, 2013b]. We now consider the influence of vertical fluxes on the euphotic layer P budget.

Previous studies reported eddy diffusivity (Kz) values measured at the base of the thermocline during this sampling campaign [*Tweddle et al.,* 2013; *Palmer et al.,* 2013]. Where these corresponded to our sampling times and locations, the K_z values were applied to estimate nutrient fluxes. Where corresponding values were not available, a derived mean value of $9.3 \times 10^{-4} \pm 7.0 \times 10^{-4}$ m^2 s^{-1} was applied to calculate vertical fluxes [*Tweddle et al.,* 2013; *Palmer et al.,* 2013]. The direction of the net flux was determined by the vertical nutrient gradients, which generally became stronger during the study as stratification enhanced after the storm subsided (Figures 1b and 1c).

Fluxes were temporally interpolated where necessary to produce a best estimate of total fluxes during the 15 day sampling campaign (Figure 4). There was a clear tidal influence in the nutrient flux data, with larger fluxes during spring tides (days 187 and 202) and in particular the earlier stormy spring tide relative to the neap tide (day 192). The magnitude of downward fluxes appears to be strongly influenced by the presence or absence of OP maxima within the lower thermocline layer. For example, on days 198 and 202 the downward DOP and PPhos flux exceeded the upward DIP flux resulting in a net loss of P on those days, which corresponded to subsurface DOP and PPhos maxima in the lower thermocline roughly associated with the SCM (Figure 1c, day 202), with DOP fluxes being greater than PPhos fluxes on those days.

We estimate that 30 ± 22 mmol DIP m^{-2} (± stdev) was mixed up into the euphotic layer via diapycnal mixing during the study period. Meanwhile, 6 ± 5 mmol DOP m^{-2} (22% of the upward flux) and 8 ± 6 mmol PPhos m^{-2} (26% of the upward flux) were removed from the euphotic layer via reciprocal downward mixing across the thermocline. These flux estimates suggest that there was a net gain of 16 ± 14 mmol P m^{-2} in the euphotic layer due to diapycnal mixing across the base of the thermocline over the course of the study. This is counterintuitive as our observations show a decrease in total integrated P in the euphotic layer.

Between days 187 and 202, we observed a net decrease in euphotic layer integrated P of 5 ± 0.1 mmol P m^{-2}, and we estimated vertical nutrient flux delivered a net gain of 16 ± 14 mmol P m^{-2} to the euphotic layer. To satisfy the observed decrease in euphotic layer P, an overall loss of 21 mmol P m^{-2} must have occurred that is unaccounted for by our observations and estimates of diapycnal mixing. We suggest that this additional loss may have been via active transport, e.g., the vertical migration of feeding zooplankton may have contributed to transfer of P below the thermocline either directly or indirectly through excretion and/or fecal matter sinking out of the euphotic layer prior to remineralization [*Steinberg et al.,* 2002]. Larger particles may sink quickly out of the euphotic layer independently of diapycnal mixing which may have significantly contributed to vertical transfers of nutrients. There may have also been lateral advection of surface waters away from the Jones Bank region.

4. Summary

Enhanced vertical mixing associated with the storm and spring tide at Jones Bank drove an enhanced vertical diapycnal DIP flux into the euphotic layer. The result was a P pool dominated by DIP on day 187 (Figures 3a–3c). Over the following 15 days we observed an overall decrease in P content in the euphotic layer, a drawdown of DIP and PPhos, and an accumulation of DOP, which dominated the phosphorus pool by day 202 (Figures 3a–3c).

During the 15 day study the net direction of diapycnal fluxes across the base of the thermocline was upwards, i.e., DIP was supplied to the euphotic layer in excess of downward mixing of DOP and PPhos (Figure 4). However, when there were subsurface DOP and PPhos maxima in the lower thermocline (Figure 1c), downward OP fluxes exceeded upward DIP fluxes. Such maxima often coincided with particularly pronounced SCM features. In the latter stages of our study, the removal of DOP-rich DOM from the euphotic layer via diapycnal mixing exceeded the equivalent export as PPhos (Figure 4). This is likely to be more representative of typical summertime shelf sea conditions as compared to the post-storm period where PPhos fluxes exceeded DOP fluxes.

Preferential release of P relative to C and N in the particulate phase made the POM pool increasingly P poor relative to C but also influenced the DOM pool, which became increasingly P rich relative to C. This implies that after the storm the downward DOM fluxes were more efficient than down POM fluxes at removing C relative to P from the euphotic layer, but that downward PPhos fluxes became increasingly efficient at removing more C relative to P than the equivalent downward DOP flux by the end of the study. The stoichiometry of the OM being mixed below the thermocline after the storm suggests that P removal from the euphotic layer is more efficient relative to N and C. As N is the limiting nutrient it is likely recycled more vigorously and retained in the euphotic layer to sustain production.

The form in which nutrients are transferred from the euphotic layer to below the thermocline, either POM or DOM, has an inherent influence over the stoichiometry of nutrient distributions through the water column. If P-rich DOM is exported below the thermocline during typical summer mixing conditions, then the nutrient pool in the bottom mixed layer (BML) may become increasingly P replete relative to N. Mixing down of POM during and after productive mixing events may act to redress this offset, as POM has higher carbon and nitrogen content relative to phosphorus.

Acknowledgments

Data, protocols, methods, and derived data products are available from the corresponding author upon request. This work was supported by NERC grant NE/F001983/1 awarded to J. Sharples and NE/K002007/1 awarded to J. Sharples, C. Mahaffey, and G. Wolff. We thank colleagues and crew on *RRS James Cook* (cruise JC025), the British Oceanographic Data Centre for providing DOC/DON data (data originator S. McNeil), and S. Blackbird for conducting C and N analysis. The authors would like to thank two anonymous reviewers and the Editor (P.Stratton) for their constructive comments that improved the paper.

Peter Strutton thanks two anonymous reviewers for their assistance in evaluating this paper.

References

Ammerman, J. W. (1993), Microbial cycling of inorganic and organic phosphorus in the water column, in *Handbook of Methods in Aquatic Microbial Ecology*, edited by P. F. Kemp et al., pp. 649–660, Lewis Publishers, Boca Raton, Fla.

Antia, A. N. (2005), Solubilization of particles in sediment traps: Revising the stoichiometry of mixed layer export, *Biogeosciences*, *2*, 189–204, doi:10.5194/bg-2-189-2005.

Azam, F., T. Fenchel, J. G. Field, J. S. Gray, L. A. Meyer-Reil, and F. Thingstad (1983), The ecological role of water-column microbes in the sea*, *Mar. Ecol. Prog. Ser.*, *10*, 257–263.

Benitez-Nelson, C. R. (2000), The biogeochemical cycling of phosphorus in marine systems, *Earth Sci. Rev.*, *51*, 109–135.

Carlson, C. A. (2002), Production and removal processes, in *Biogeochemistry of Marine Dissolved Organic Matter*, edited by D. A. Hansell and C. A. Carlson, pp. 91–151, Academic Press, Santa Barbara, Calif.

Conan, P., et al. (2007), Partitioning of organic production in marine plankton communities: The effects of inorganic nutrient ratios and community composition on new dissolved organic matter, *Limnol. Oceanogr.*, *52*(2), 753–765.

Davidson, K., L. C. Gilpin, R. Pete, D. Brennan, S. McNeill, G. Moschonas, and J. Sharples (2013), Phytoplankton and bacterial distribution and productivity on and around Jones Bank in the Celtic Sea, *Prog. Oceanogr.*, *117*, 48–63.

Faul, K. L., A. Paytan, and M. L. Delaney (2005), Phosphorus distribution in sinking oceanic particulate matter, *Mar. Chem.*, *97*, 307–333.

Hickman, A. E., C. M. Moore, J. Sharples, M. I. Lucas, G. H. Tilstone, V. Krivtsov, and P. Holligan (2012), Primary production and nitrate uptake within the seasonal thermocline of a stratified shelf sea, *Mar. Ecol. Prog. Ser.*, *463*, 39–57.

Hopkinson, C. S., B. Fry, and A. L. Nolin (1997), Stoichiometry of dissolved organic matter dynamics on the continental shelf of the northeastern U.S.A., *Cont. Shelf Res.*, *17*(5), 473–489.

Hydes, D. J., et al. (2001), Supply and demand of nutrients and dissolved organic matter at and across the NW European shelf break in relation to hydrography and biogeochemical activity, *Deep Sea Res., Part II*, *48*(14), 3023–3047.

Karl, D. M., K. M. Björkman, J. E. Dore, L. Fujieki, D. V. Hebel, T. Houlihan, R. M. Letelier, and L. M. Tupas (2001), Ecological nitrogen-to-phosphorus stoichiometry at station ALOHA, *Deep Sea Res., Part II*, *48*, 1529–1566.

Lønborg, C., and X. Alvarez-Salgado (2012), Recycling versus export of bioavailable dissolved organic matter in the coastal ocean and efficiency of the continental shelf pump, *Global Biogeochem. Cycles*, *26*, GB3018, doi:10.1029/2012GB004353.

Martiny, A. C., C. T. A. Pham, F. W. Primeau, J. A. Vrugt, J. K. Moore, S. A. Levin, and M. W. Lomas (2013), Strong latitudinal patterns in the elemental ratios of marine plankton and organic matter, *Nat. Geosci.*, *6*, 279–283.

Palmer, M. R., M. E. Inall, and J. Sharples (2013), The physical oceanography of Jones Bank: A mixing hotspot in the Celtic Sea, *Prog. Oceanogr.*, *117*, 9–24.

Paytan, A., and K. McLaughlin (2007), The oceanic phosphorus cycle, *Chem. Rev.*, *107*(2), 563–576, doi:10.1021/cr0503613.

Pemberton, K., A. P. Rees, P. I. Miller, R. Raine, and I. Joint (2004), The influence of water body characteristics on phytoplankton diversity and production in the Celtic Sea, *Cont. Shelf Res.*, *24*(17), 2011–2028.
Redfield, A. C., B. H. Ketchum, and F. A. Richards (1963), The influence of organisms on the composition of sea-water, in *The Sea*, edited by M. N. Hill, pp. 26–77, Wiley, New York.
Reynolds, S., C. Mahaffey, V. Roussenov, and R. G. Williams (2014), Evidence for production and lateral transport of dissolved organic phosphorus in the eastern subtropical North Atlantic, *Global Biogeochem. Cycles*, *28*, 805–824, doi:10.1002/2013GB004801.
Ruttenberg, K. C., and S. T. Dyhrman (2005), Temporal and spatial variability of dissolved organic and inorganic phosphorus, and metric of phosphorus bioavailability in an upwelling-dominated coastal system, *J. Geophys. Res.*, *110*, C10S13, doi:10.1029/2004JC002837.
Ruttenberg, K. C., and S. T. Dyhrman (2012), Dissolved organic phosphorus production during simulated phytoplankton blooms in a coastal upwelling system, *Front. Microbiol.*, *3*, 274, doi:10.3389/fmicb.2012.00274.
Sharples, J., et al. (2007), Spring-neap modulation of internal tide mixing and vertical nitrate fluxes at a shelf edge in summer, *Limnol. Oceanogr.*, *52*(5), 1735–1747, doi:10.4319/lo.2007.52.5.1735.
Sharples, J., B. E. Scott, and M. E. Inall (2013), From physics to fishing over a shelf sea bank, *Prog. Oceanogr.*, *117*, 1–8.
Sohm, J. A., C. Mahaffey, and D. G. Capone (2008), Assessment of relative phosphorus limitation of Trichodesmium spp. in the North Pacific and Atlantic and the North Coast of Australia, *Limnol. Oceanogr.*, *53*(6), 2495–2502.
Steinberg, D. K., S. A. Goldthwait, and D. A. Hansell (2002), Zooplankton vertical migration and the active transport of dissolved organic and inorganic nitrogen in the Sargasso Sea, *Deep Sea Res., Part I*, *49*(8), 1445–1461, doi:10.1016/S0967-0637(02)00037-7.
Thomas, H., Y. Bozec, K. Elkalay, and H. J. W. de Baar (2004), Enhanced open ocean storage of CO2 from shelf sea pumping, *Science*, *304*, 1005–1008, doi:10.1126/science.1095491.
Tweddle, J. F., J. Sharples, M. R. Palmer, K. Davidson, and S. McNeill (2013), Enhanced nutrient fluxes at the shelf sea seasonal thermocline caused by stratified flow over a bank, *Prog. Oceanogr.*, *117*, 37–47.
Wetz, M. S., and P. A. Wheeler (2003), Production and partitioning of organic matter during simulated phytoplankton blooms, *Limnol. Oceanogr.*, *48*(5), 1808–1817.
Williams, C. A., J. Sharples, M. Green, C. Mahaffey, and T. P. Rippeth (2013a), The maintenance of the subsurface chlorophyll maximum in the western Irish Sea, *Limnol. Oceanogr. Fluids Environ.*, *3*, 61–73.
Williams, C. A., J. Sharples, C. Mahaffey, and T. Rippeth (2013b), Wind-driven nutrient pulses to the subsurface chlorophyll maximum in seasonally stratified shelf seas, *Geophys. Res. Lett.*, *40*, 5467–5472, doi:10.1002/2013GL058171.
Wollast, R. (1998), Evaluation and comparison of the global carbon cycle in the coastal zone and in the open ocean, in *The Sea*, vol. 10, edited by K. H. Brink and A. R. Robinson, pp. 213–252, John Wiley, New York.
Yamamuro, M., and H. Kayanne (1995), Rapid direct determination of organic-carbon and nitrogen in carbonate-bearing sediments with a yanaco mt-5 chn analyzer, *Limnol. Oceanogr.*, *40*, 1001–1005.